Measurement of proton relaxation rates in proteins

Benoit Boulat* and Geoffrey Bodenhausen**

Section de Chimie, Université de Lausanne, Rue de la Barre 2, CH-1005 Lausanne, Switzerland

SUMMARY

Five different types of experiment are described which make it possible to measure various relaxation rates of selected protons in crowded spectra of macromolecules such as proteins: longitudinal spin-lattice relaxation rates $\rho = 1/T_1$, transverse relaxation rates $\rho^t = 1/T_2$ measured under conditions of free precession, transverse relaxation rates $\rho^t_{LOCK} = 1/T_{1\rho}$ measured under conditions of spin-locking, and transverse relaxation rates $\rho^{DQC} = 1/T_2^{DQC}$ and $\rho^{ZQC} = 1/T_2^{ZQC}$ of double- and zero-quantum coherences. The surprisingly large discrepancy between the transverse rates ρ^t and ρ^t_{LOCK} is discussed in detail. To separate overlapping proton signals, the experimental schemes involve one or several magnetization transfer steps, using a doubly selective homonuclear Hartmann–Hahn method. Numerous variants of the basic ideas can be conceived, depending on the extent of signal overlap and on the topology of the networks of scalar couplings. Applications are shown to H^ϵ and H^δ of Tyr^{23}, to H^α, H^β and $H^{\beta'}$ of Cys^{30}, and to H^α and H^β of Ala^{24} in bovine pancreatic trypsin inhibitor (BPTI).

INTRODUCTION

In recent years, there has been much interest in the measurement and interpretation of NMR relaxation rates of biological macromolecules such as proteins and nucleic acids (Kay et al., 1989; Clore et al., 1990; Palmer et al., 1991a,b; Peng et al., 1991a,b; Brüschweiler and Ernst, 1992; Peng and Wagner, 1992). By and large, attention has been focused on ^{13}C and ^{15}N relaxation rates, partly because these parameters are simpler to interpret than proton relaxation rates, and partly because the ^{13}C and ^{15}N spectra are usually well resolved, or, if they are not, because the signals can be readily separated with the help of two- or multidimensional heteronuclear correlation methods. While a considerable amount of data on ^{13}C and ^{15}N relaxation rates has been accumulated, and while great progress has been made in the interpretation of these rates in terms of

*Present address: Scripps Research Institute, 10666 North Torrey Pines Road, La Jolla, CA 92037, U.S.A.
**To whom correspondence should be addressed.

molecular mobility, the measurement of *proton* relaxation data has been largely neglected so far, except of course for the ubiquitous measurement of cross-relaxation rates σ_{AX} by various Overhauser methods. The fact that the measurement of proton relaxation rates has been neglected is no accident: (1) extensive signal overlap makes traditional one-dimensional methods such as inversion- recovery impractical; (2) the presence of homonuclear couplings implies that spin-echoes are modulated, thus making it difficult to measure transverse relaxation rates under conditions of free precession; (3) measurement of transverse relaxation under spin-locked conditions by conventional $T_{1\rho}$ methods is complicated by coherence transfer processes through scalar couplings; (4) the spectral widths of double-quantum spectra of macromolecules are so large that it is difficult to obtain sufficient digital resolution to estimate the line widths and hence the transverse relaxation rates of double- quantum coherences. Finally, it is clear that proton relaxation rates tend to be more difficult to interpret. In many cases, the time dependence of the decay or recovery of proton magnetization is determined by multiexponential laws, so that it is an oversimplification to speak of simple 'rates'. We shall nevertheless use this parlance, since in many cases the initial rates are a good approximation to the true self-relaxation rates $\rho = 1/T_1$, $\rho^t = 1/T_2$ or $\rho^t_{LOCK} = 1/T_{1\rho}$ (Vold and Vold, 1976, 1978; Werbelow and Grant, 1977; Kowalewski, 1990). Proton relaxation may be influenced by a manifold of homonuclear dipole–dipole interactions, by chemical shift anisotropy, by chemical exchange and slow motion, and by various cross-correlation effects. We are convinced that the very richness of proton relaxation data constitutes a powerful motivation to develop methods to make their measurement more readily accessible.

SELECTIVE APPROACHES

The basic idea that we have pursued is that one should 'interrogate' the system in a selective manner, one proton after the other. In the rigorous terminology that is employed by relaxation experts (Vold and Vold, 1978) one should actually speak of semi-selective experiments, since we excite and observe entire multiplets rather than individual lines. At first sight, this approach may appear rather cumbersome and time-consuming for macromolecules. Surprisingly, however, selective methods can be very time effective, since the individual experiments can be carried out very quickly, provided that the proton spectra have been previously assigned with the usual multi-dimensional techniques. We do not, of course, propose to measure the relaxation behaviour of *all* protons in a macromolecule. We merely suggest to compare the rates of some significant subset of protons, such as the rates of all H^α protons, or those of all aromatic tyrosine protons. Thus we may selectively investigate certain types of motional processes.

In this paper, we describe five different types of experiment which make it possible to measure various proton relaxation rates in a selective fashion. Most of the constituent building blocks of our experiments have been described elsewhere (Konrat et al., 1991; Boulat et al., 1992; Burghardt et al., 1992; Nicula and Bodenhausen, 1993), but many of the combinations are novel, and almost none have been applied to proteins until now. In proton NMR spectra of biological macromolecules, the signals usually overlap severely, so that it is necessary to separate interfering signals. This can be achieved by one or several magnetization transfer steps using the doubly selective homonuclear Hartmann–Hahn (HOHAHA) method (Konrat et al., 1991). In the schematic pulse sequences shown in Figs. 1 and 2, the sinusoidally modulated bursts of radiofrequen-
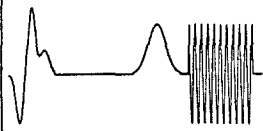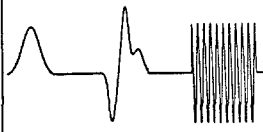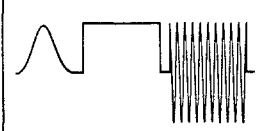
Tyrosine 23 in BPTI			
RATES	ϵ	δ	EXPERIMENTS
ρ	2.3	3.8	
ρ^t	13.5	18.3	
ρ^t_{LOCK}	6.4	17.5	
ρ^{DQC}	45		
ρ^{ZQC}	39		

Fig. 1. Proton relaxation parameters in Tyr[23] in BPTI at 327 K. The appropriate pulse sequences are shown schematically to the right, and the parameters that can be determined to the left, with the longitudinal self-relaxation rate $\rho = 1/T_1$, the transverse self-relaxation rate $\rho^t = 1/T_2$ measured under conditions of free precession, the transverse self-relaxation rate $\rho^t_{LOCK} = 1/T_{1\rho}$ measured in the presence of a spin-locking field, and the decay rates ρ^{DQC} and ρ^{ZQC} of double- and zero-quantum coherences. The rates for H^ϵ and H^δ in the central columns are given in s^{-1}.

cy irradiation represent such transfer steps. Their mechanism has been described elsewhere (Konrat et al., 1991; Zwahlen et al., 1992, 1993; Vincent et al., 1992). Suffice it to say here that, provided a scalar coupling J_{AX} can be identified between the proton A under investigation and any other proton X, it is always possible to transfer transverse magnetization from A to X by irradiating both spins simultaneously with two weak, selective radiofrequency fields applied at the chemical shifts Ω_A and Ω_X. In practice, this can be done by setting the carrier frequency at $\omega_O = \frac{1}{2}(\Omega_A + \Omega_X)$ and modulating the amplitude with $\cos \omega_a t$, where $\omega_a = \frac{1}{2}(\Omega_A - \Omega_X)$. The transfer of transverse magnetization ($I_x^A \rightarrow I_x^X$) is most effective if the duration of the doubly selective irradiation fulfils the condition $\tau_{DSI} = 1/J_{AX}$. If relaxation during the doubly selective
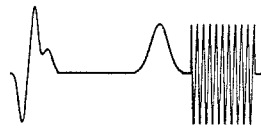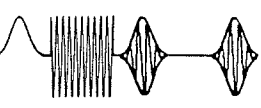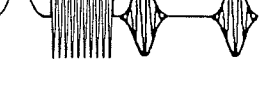
Cysteine 30 in BPTI				
RATES	α	β	β'	EXPERIMENTS
ρ	3.3	7.6	8.0	
ρ^t	11.3	14.0	17.0	
ρ^t_{LOCK}	5.1	12.3	10.3	
ρ^{DQC}	30		–	
	–	30		
ρ^{ZQC}	36		–	
	–	36		

Fig. 2. Proton relaxation parameters in Cys[30] in BPTI, presented in a format similar to Fig. 1. The rates for H^α, H^β and $H^{\beta'}$, in the central columns are given in s^{-1}. The decay rates ρ^{DQC} and ρ^{ZQC} of double- and zero-quantum coherences have only been measured for pairs of protons that have a large scalar coupling.

irradiation is fast, it is advisable to set $\tau_{DSI} < 1/ J_{AX}$. Even if the transfer is less than complete, it is still possible to obtain an accurate picture of the relaxation behaviour of the A proton. The doubly selective Hartmann–Hahn transfer allows one to separate overlapping signals completely whenever there is only one pair of scalar-coupled spins that resonate at the frequencies Ω_A and Ω_X. In practice, this is equivalent to demanding that there should not be any overlapping cross peaks between Ω_A and Ω_X in a double-quantum-filtered correlation spectrum (Piantini et al., 1982; Rance et al., 1983). If this condition is not satisfied, a complete separation can usually be achieved with several consecutive transfer steps.

Figure 1 schematically shows four pulse sequences. The first experiment is designed to measure the longitudinal spin-lattice relaxation rate ρ of a chosen spin A. The longitudinal component is first inverted ($I_z^A \rightarrow -I_z^A$) by a selective Q^3 Gaussian cascade (Emsley and Bodenhausen, 1992), allowed to recover partly during a variable relaxation interval τ_{rel}, converted into a transverse

component $(I_z^A \rightarrow I_x^A)$ by a Gaussian pulse with a 270° nutation angle (Emsley and Bodenhausen, 1989), which is finally transferred to transverse magnetization of a scalar-coupled neighbour $(I_x^A \rightarrow I_x^X)$ in the doubly selective irradiation period τ_{DSI} (Konrat et al., 1991). In this manner, the amplitude of the X-spin signal is proportional to the I_z^A component at the end of the τ_{rel} delay.

The second sequence in Fig. 1 is designed to determine transverse relaxation rates ρ^t measured under conditions of free precession. The initial selective pulse, again a Gaussian pulse with a 270° nutation angle, excites transverse magnetization of a chosen multiplet $(I_z^A \rightarrow I_x^A)$, which after a period $\frac{1}{2}\tau_{rel}$ of free precession is refocused $(I_y^A \rightarrow -I_y^A, I_x^A \rightarrow I_x^A)$ by a selective Q^3 Gaussian cascade to form an echo. Because the refocusing is selective, the echo is *not* modulated by scalar couplings (Emsley et al., 1990). At the top of the echo, the (in-phase) transverse magnetization I_x^A is 'picked up' (actually spin-locked) by one of the sidebands of the modulated radiofrequency field, and transferred through the Hartmann–Hahn effect to a scalar- coupled neighbour $(I_x^A \rightarrow I_x^X)$.

The third method of Fig. 1 shows a variant designed to measure transverse relaxation rates ρ^t_{LOCK} measured under conditions of spin-locking. In this case, the magnetization is initially excited by a Gaussian pulse with a 270° nutation angle and then locked by a weak, selective radiofrequency field (Burghardt et al., 1992). After partial decay of the magnetization of spin A during a variable spin-locking interval τ_{rel} with *monochromatic* irradiation at Ω_A, the residual magnetization is locked by one of the sidebands of the *modulated* radiofrequency field, and transferred to a scalar coupled neighbour $(I_x^A \rightarrow I_x^X)$.

Finally, the fourth sequence in Fig. 1 shows how to measure transverse relaxation rates ρ^{DQC} and ρ^{ZQC} of double- and zero-quantum coherences. We have given a detailed description of these experiments elsewhere (Nicula and Bodenhausen, 1993). Suffice it to say here that transverse magnetization (single-quantum coherence) of a chosen spin A is initially excited with a 270° Gaussian pulse, and then converted into antiphase magnetization $(I_x^A \rightarrow 2I_y^A I_z^X -2I_z^A I_y^X)$ during a doubly selective irradiation interval of duration $\tau_{DSI} \approx (2J_{AX})^{-1}$. These antiphase terms are converted by a modulated 270° Gaussian pulse into double- or zero-quantum coherences, which are then allowed to precess during the subsequent evolution period t_1. These coherences are reconverted into observable magnetization by the last 270° Gaussian pulse, which is also modulated. Suitable phase cycling allows one to focus attention on either double- or zero-quantum terms. Because the method is selective, it is possible to have a very narrow spectral width in the ω_1 dimension, so that it is easy to fulfil the condition $t_1^{max} > > T_2(DQC)$, $T_2(ZQC)$ to avoid truncation. In a two-spin subsystem, there is no multiplet structure in the zero- or double-quantum dimension. As a result, the full line width at half-height $\Delta\nu$ (expressed in Hz) gives a reasonably accurate measure of the relaxation rates $(T_2^{MQC} = 1/\pi\Delta\nu$ or $\rho^{MQC} = \pi\Delta\nu)$. Because these rates turn out to be rather fast in our experimental examples, it does not seem necessary to refocus the inhomogeneous dephasing of the double- or zero- quantum coherences, although this can in principle be done by inserting a modulated Gaussian cascade Q^3 in the middle of the evolution period, provided that relaxation is not too fast. This would also refocus evolution due to scalar interactions with passive spins, which give rise to multiplets in the ω_1 dimension of double- and zero-quantum spectra of systems with three and more spins.

It is possible to conceive numerous variants of the basic methods shown in Fig. 1, depending on how severely the signals overlap. In particular, the experiments can be modified by first

exciting magnetization I_x^X of a scalar-coupled neighbour X, and then 'injecting' this magnetization $(I_x^X \rightarrow I_x^A)$ into the spin A of interest by the doubly selective HOHAHA method (Zwahlen et al., 1992) or by other pulse sequences (Müller et al., 1991). One may then continue with any one of the pulse sequences illustrated in Fig. 1. The choice should be made according to the topology of the network under investigation.

MATERIALS AND METHODS

A sample of 20 mg lyophilized BPTI was dissolved in about 0.5 ml 99.9% D_2O. All chemical shifts are referenced to the methyl resonance at 0 ppm of 3-(trimethylsilyl)-1-propanesulfonic acid. All NMR spectra were recorded at 327 K on a Bruker MSL 300 spectrometer, except the double- and zero-quantum spectra, which were recorded at the same temperature on a Bruker AM 400 spectrometer. Both spectrometers were equipped with process controllers for digital phase shifting and selective excitation units designed by Oxford Research Systems. Double-quantum filtered correlation experiments (Piantini et al., 1982; Rance et al., 1983) and doubly selective homonuclear Hartmann–Hahn (HOHAHA) experiments (Konrat et al., 1991) were used to confirm the assignments of the resonances (Wagner and Wüthrich, 1982). The other experimental methods are described above. The 270° Gaussian pulses and the Q^3 Gaussian cascades used for inversion or refocusing (Emsley and Bodenhausen, 1992) were typically of 30 ms duration each. The radiofrequency amplitudes were adjusted for maximum excitation and inversion, respectively. The length τ_{DSI} of the doubly selective irradiation period was adjusted empirically for maximum transfer. All free induction decays were multiplied prior to Fourier transformation by a Lorentz-to-Gauss window function with an exponential line broadening factor of -1.5 and a Gaussian broadening factor of 0.05. Further details are given in the figure captions.

RESULTS AND DISCUSSION

Figures 1 to 3 show the results of selective measurements of the H^ε and H^δ protons of Tyr^{23}, of the H^α, H^β and $H^{\beta'}$ protons of Cys^{30}, and of the H^σ and H^β protons of Ala^{24} in bovine pancreatic trypsin inhibitor (BPTI). Except for the double- and zero-quantum coherences, all relaxation rates were determined from the initial slopes of semi-logarithmic plots derived from signals such as those shown in Figs. 4 to 7. The double- and zero-quantum relaxation rates were estimated from the line widths, although it could not be ascertained that the lines have simple Lorentzian shapes. The experiments were repeated at least three times (and in some cases ten times); the deviations were in the order of ± 0.5 s^{-1}.

The longitudinal self-relaxation rates ρ in Figs. 1–3 cover a surprisingly wide range. The difference between the ρ rates of H^ε and H^δ in Tyr^{23} can be explained qualitatively by noting that H^δ is much more exposed than H^ε to the fluctuating dipolar fields arising from the H^β and $H^{\beta'}$ protons of the same amino acid. For the Cys^{30} residue, the large difference between the ρ rates of H^β and $H^{\beta'}$ on the one hand, and the ρ rate of H^α on the other, obviously reflects the close proximity of H^β and $H^{\beta'}$.

The ρ^t and ρ^t_{LOCK} rates measured in Tyr^{23} (see Fig. 1) deserve a more detailed discussion. It is remarkable that the rates ρ^t and ρ^t_{LOCK} of H^ε are very different, while those of H^δ on the same ring are rather similar. We shall discuss two different hypotheses to explain these facts. First, a slow

Alanine 24 in BPTI			
RATES	α	β	EXPERIMENTS
ρ	2.1	2.9	
ρ^t	5.4	5.6	
ρ^t_{LOCK}	4.9	5.2	

Fig. 3. Proton relaxation parameters in Ala[24] in BPTI, presented in a format similar to Fig. 1. The rates for H^α and H^β in the central column are given in s^{-1}. The decay rates of double- and zero-quantum coherences have not been measured in this system.

ring-flip motion could contribute to the spectral densities at low frequencies. Such a motion could help to explain the discrepancy between ρ^t and ρ^t_{LOCK} of H^ϵ, which should depend on the difference $\Omega(H^\epsilon) - \Omega(H^{\epsilon'})$ of the (unknown) chemical shifts in the static low temperature limit. The same slow ring-flip motion need not lead to a significant discrepancy between the rates ρ^t and ρ^t_{LOCK} of H^δ, since it is quite possible that $\Omega(H^\delta) - \Omega(H^{\delta'})$ is much smaller than $\Omega(H^\epsilon) - \Omega(H^{\epsilon'})$ in the low temperature limit. Indeed, such a trend is verified in Tyr[35] in BPTI, which rotates so slowly that all four chemical shifts are resolved (Wagner and Wüthrich, 1982; Wagner et al., 1985). For Tyr[23], the rate of the ring-flip motion has been estimated to be 300 s^{-1} at 309 K (Wagner et al., 1987) and at our temperature of 327 K it is probably too fast to affect the line width. If slow ring-flip motion was responsible for the discrepancy between ρ^t and ρ^t_{LOCK} of H^ϵ in Tyr[23], the transverse relaxation rate ρ^t_{LOCK} should depend on the nutation frequency $\omega_e = \gamma B_1$ of the applied field (Blicharski, 1972; Peng et al., 1991a). We have therefore measured the rate ρ^t_{LOCK} of H^ϵ of Tyr[23] as a function of the amplitude of the locking field. For $37 < \omega_e/2\pi < 77$ Hz, we have not found any significant differences. Unfortunately, the experimentally accessible range is limited in our experiments by the requirement that the radiofrequency irradiation must remain selective. Further evidence against a slow-motion hypothesis is provided by Cys[30] (Fig. 2), where it would be difficult to conceive some form of slow motion to explain why the rates ρ^t and ρ^t_{LOCK} of H^α are so different, while those of H^β are rather similar.

We can formulate a second hypothesis to explain the striking discrepancy between the rates ρ^t and ρ^t_{LOCK} of H^ϵ. It has been shown (Goldman, 1984; Palmer et al., 1991a; Peng et al., 1991b;
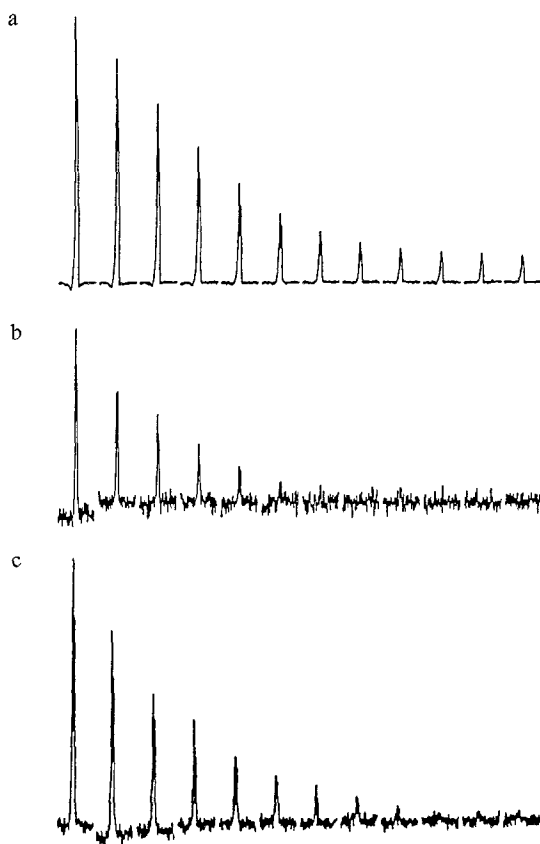
342

Fig. 4. Spectra used to determine the transverse relaxation rates in Tyr[23] in BPTI: (a) ρ^t of H^ϵ, the signal of H^ϵ being recorded directly, (b) ρ^t of H^δ, the signal of H^δ being recorded indirectly with the help of a HOHAHA transfer onto H^ϵ, and (c) ρ^t_{LOCK} of H^δ, also observed indirectly through HOHAHA. In (a) and (b), the interval between the initial 270° Gaussian and the Q^3 refocusing pulse was incremented from 0 to 110 ms in steps of 10 ms, so that the total free precession period between the initial excitation and the top of the echo was incremented from 0 to 220 ms. In (c), the spin-locking duration was incremented from 0 to 220 ms. The number of scans was 16 in each case. Note that the sensitivity of the signals in (b) and (c) recorded after HOHAHA transfer is poorer than in (a), where the signals were observed directly.
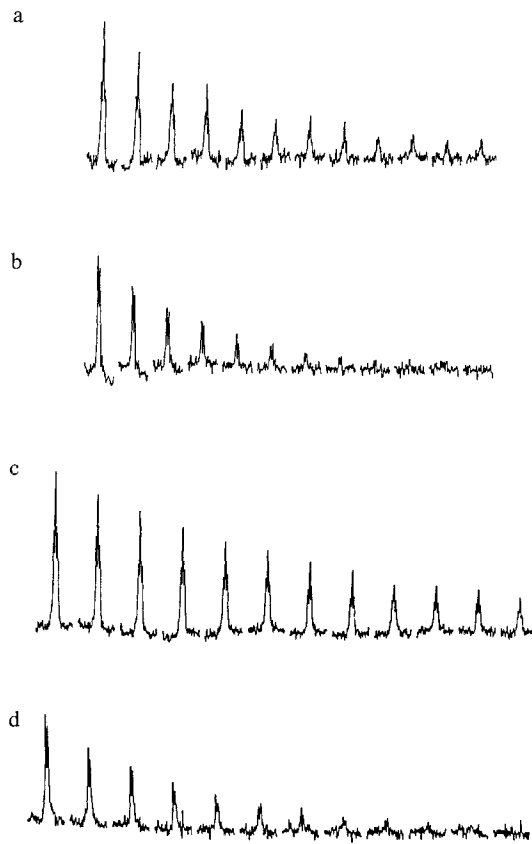
Fig. 5. Spectra used to determine the transverse relaxation rates in Cys[30] in BPTI: (a) ρ^t of H^α, the H^α signals being recorded indirectly with the help of a HOHAHA transfer onto H^β, (b) ρ^t of H^β, the signals being transferred onto H^α, (c) ρ^t_{LOCK} of H^α, observed indirectly through transfer to H^β, and (d) ρ^t_{LOCK} of H^β, observed indirectly through HOHAHA transfer to H^α. The relaxation intervals were incremented from 0 to 220 ms. The number of scans was 128.

Peng and Wagner, 1992) that antiphase terms such as $2I_x{}^A I_z{}^X$ or $2I_y{}^A I_z{}^X$ may have a different relaxation rate than in-phase coherences $I_x{}^A$ or $I_y{}^A$. This effect is particularly pronounced when spin X (i.e., the scalar coupling partner of spin A) experiences, in addition to the A–X interaction, further dipolar interactions X–M, X–M′, X–M″ ... to other spins M, M′, M″, ... (Bax et al., 1990). Neglecting long-range dipole– dipole interactions A–M, A–M′, A–M″,..., cross-correla-

tions and chemical shift anisotropy terms, the transverse relaxation rates of in-phase and antiphase single- quantum coherences are (Lipari and Szabo, 1982; Peng and Wagner, 1992):

$$\rho^t(I_x^A) = \rho^t(I_y^A) = \rho^t_{in} = \gamma^4\hbar^2(8r_{AX}^6)^{-1}\ \{5J_{AX}(0) + 9J_{AX}(\omega_0) + 6J_{AX}(2\omega_0)\} \tag{1}$$

$$\rho^t(2I_x^A I_z^X) = \rho^t(2I_y^A I_z^X) = \rho^t_{anti} = \tag{2}$$

$$\gamma^4\hbar^2(8r_{AX}^6)^{-1}\ \{5J_{AX}(0) + 3J_{AX}(\omega_0) + 6J_{AX}(2\omega_0)\} + \rho_{MX} + \rho_{M'X} + \rho_{M''X} + \ldots$$

where

$$\rho_{MX} = \gamma^4\hbar^2(4r_{MX}^6)^{-1}\ \{J_{MX}(0) + 3J_{MX}(\omega_0) + 6J_{MX}(2\omega_0)\}. \tag{3}$$

In these expressions, γ is the gyromagnetic ratio, while r_{AX} and r_{MX} are the internuclear distances. The spectral density function $J_{AX}(\omega)$, which describes the fluctuations of the orientations of the vector r_{AX}, is defined by

$$J_{AX}(\omega) = 2 \int_0^\infty G_{AX}(\tau) \cos \omega\tau\ d\tau. \tag{4}$$

with the autocorrelation function

$$G_{AX}(\tau) = (1/5) < P_2(\mathbf{u}_{AX}(0) \cdot \mathbf{u}_{AX}(\tau)) > = (1/5) < P_2\ (\cos \theta_{AX}(0,\tau)) > \tag{5}$$

where $\mathbf{u}_{AX}$ is a unit vector parallel to $\mathbf{r}_{AX}$, and where $P_2\ (\cos \theta_{AX}) = \frac{1}{2}(3\cos^2\theta_{AX} - 1)$. The functions $J_{MX}(\omega)$ and $G_{MX}(\tau)$ are defined by analogy. The expressions of our Eqs. 1 and 2 have been adapted to homonuclear systems from Eqs. 7 and 11 in the work of Peng and Wagner (1992).

Now consider the difference between the decay rates of the antiphase and in-phase terms:

$$\Delta\rho^t = \rho^t_{anti} - \rho^t_{in} = - 6\gamma^4\hbar^2(8r_{AX}^6)^{-1}J_{AX}(\omega_0) + \rho_{MX} + \rho_{M'X} + \rho_{M''X} + \ldots \tag{6}$$

In large molecules in the slow motion limit, the $J_{AX}(\omega_0)$ term will be small, and the difference $\Delta\rho^t$ will be largely determined by the terms $\rho_{MX} + \rho_{M'X} + \rho_{M''X} + \ldots$, so that antiphase coherences of spin A will decay faster than in-phase coherences. Note that for spin A the difference $\Delta\rho^t$ is enhanced if the scalar coupling partner X is exposed to fluctuating dipolar fields originating in remote spins M, M', M'',... This is reminiscent of scalar relaxation of the second kind (London, 1990). On the other hand, if there are not any nuclei M, M', M'', ... that are close enough to play a significant role, and if the motion is fast enough for $J_{AX}(\omega_0)$ to be non-vanishing, the difference $\Delta\rho^t$ is negative, so that the in-phase terms decay faster.

The implications of this remarkable situation deserve a thorough discussion. If we measure transverse decays under conditions of free precession, we must consider the simultaneous effects of scalar coupling (which converts I_x^A into $2I_y^A I_z^X$ and vice versa) and relaxation, which leads to an attenuation of the I_x^A and $2I_y^A I_z^X$ terms with the rates of Eqs. 1 and 2. This is best discussed in an interaction representation (doubly rotating frame, Zwahlen et al., 1993) where both chemical shifts have been removed and only the scalar coupling remains in the Hamiltonian:
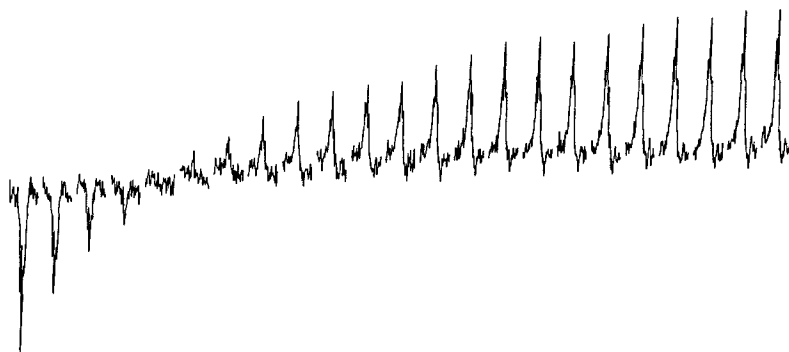
$$H = \pi J2I_z^A I_z^X. \tag{7}$$

Fig. 6. Measurement of the longitudinal relaxation rate ρ of $H^{\beta'}$ of Cys[30] in BPTI, with the relaxation period incremented from 0 to 440 ms in 20 ms steps. The signals were transferred to H^β of the same residue by the doubly selective HOHAHA method. The equilibrium value was obtained by skipping the initial inversion pulse. The number of scans was 256.

In the basis $\{I_x^A, 2I_y^A I_z^X\}$, the time dependence of the density operator is given by the Liouville equation:

$$\sigma(t) = \exp\{Lt\}\ \sigma(0) \tag{8}$$

with

$$L = \begin{pmatrix} -\rho_{in}^t & \pi J \\ -\pi J & -\rho_{anti}^t \end{pmatrix} \tag{9}$$

This matrix can be diagonalized analytically so that one can obtain an explicit description of the evolution. We neglect longitudinal cross relaxation to further spins, which would give rise to terms such as $2I_y^A I_z^M$ and therefore would require an extension of the dimension of the operator basis. The chemical shift terms do not appear in the equations because of the interaction representation, but of course they do play a role in the experiment. We consider a simple spin-echo method with a single refocusing pulse applied at $\frac{1}{2}\tau$, i.e. in the middle of the relaxation delay. Just before the refocusing pulse, we obtain:

$$\sigma(\tfrac{1}{2}\tau) = I_x^A\ (-i/2C)\ [(\Delta\rho^t + iC)\exp\{-\lambda_1 \tfrac{1}{2}\tau\} - (\Delta\rho^t - iC)\exp\{-\lambda_2 \tfrac{1}{2}\tau\}]$$
$$+ 2I_y^A I_z^X\ (i\pi J/C)\ [\exp\{-\lambda_1 \tfrac{1}{2}\tau\} - \exp\{-\lambda_2 \tfrac{1}{2}\tau\}] \tag{10}$$

where $\Delta\rho^t = \rho_{anti}^t - \rho_{in}^t$, $C = [(2\pi J)^2 - (\Delta\rho^t)^2]^{1/2}$, and where the eigenvalues are:

$$\lambda_1 = \tfrac{1}{2}(\Sigma\rho^t + iC)$$
$$\lambda_2 = \tfrac{1}{2}(\Sigma\rho^t - iC) \tag{11}$$

with $\Sigma\rho^t = \rho_{anti}^t + \rho_{in}^t$. If we neglect relaxation during the selective Q^3 refocusing pulse, its effect is equivalent to a simple π rotation about the x-axis. Thus the $2I_y^A I_z^X$ term changes sign just after
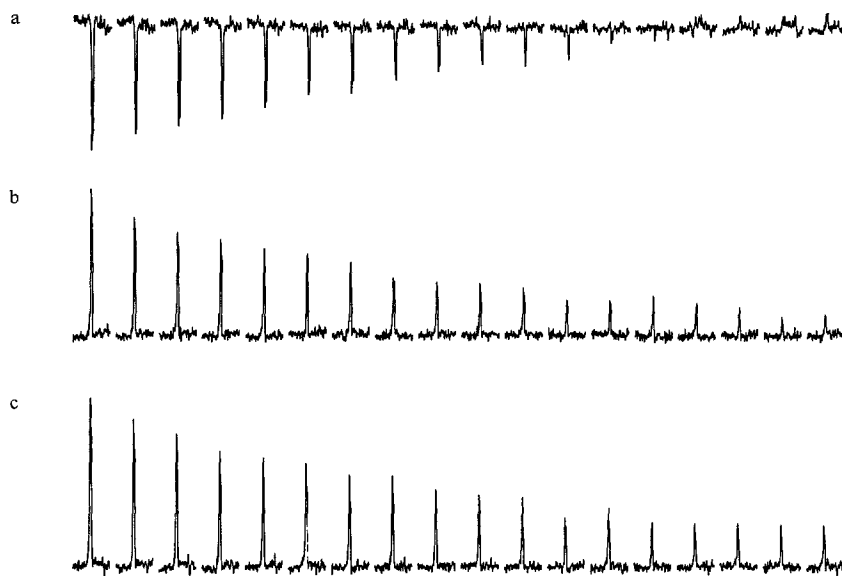
Fig. 7. Spectra used to determine the rates ρ, ρ^t, and ρ^t_{LOCK} of H^α of Ala^{24}. The relaxation intervals were incremented from 0 to 220 ms.

the Q^3 pulse, while the I_x^A term remains invariant. After the refocusing interval we obtain at the time of the echo:

$$\sigma(\tau) = I_x^A \, (2\pi J/C)^2 \exp\{ - \tfrac{1}{2}\Sigma\rho^t\tau\} \, [1 - \Delta\rho^t(\Delta\rho^t \cos C\tau - C \sin C\tau)/(4\pi^2 J^2)]$$
$$- 2I_y^A I_z^X \, (2\pi J/C^2) \, \Delta\rho^t \exp\{ - \tfrac{1}{2}\Sigma\rho^t\tau\} \, [1 - \cos C\tau] \tag{12}$$

Fortunately, $\Delta\rho^t$ is likely to be much smaller than $2\pi J$, scalar couplings being typically on the order of $J \approx 10$ Hz, so that $(2\pi J/C)^2 \approx 1$ and $2\pi J/C^2 \approx 1/2\pi J \approx 0.015$, and we can safely assume that $\Delta\rho^t/(2\pi^2 J^2) \approx 0$. Therefore, the expectation value $< 2I_y^A I_z^X >$ is always vanishingly small at the time of the echo, and Eq. 12 may be simplified to give

$$\sigma(\tau) \approx I_x^A \exp\{ - \tfrac{1}{2}\Sigma\rho^t\tau\} \tag{13}$$

Thus we observe a *monoexponential* 'T$_2$ decay' with a decay rate $\tfrac{1}{2}\Sigma\rho^t = \tfrac{1}{2}(\rho^t_{anti} + \rho^t_{in})$. If $\Delta\rho^t = 0$, that is to say if X is *not* exposed to any dipolar fields emanating from spins M, M', ... other than A, and if we are in the slow motion limit so that the spectral density $J_{AX}(\omega_0)$ in Eq. 6 vanishes, we immediately derive from Eq. 13:

$$\sigma(\tau) \approx I_x^A \exp\{ - \rho^t\tau\} \tag{14}$$

where $\rho^t = \rho^t_{in} = \rho^t_{anti}$. The expression of Eq. 13 is generally applicable to T_2 measurements under conditions of free precession. On the other hand, the measurement of transverse decay under conditions of spin-locking yields a rate ρ^t_{LOCK} which corresponds to the decay of a pure in-phase term, which cannot be 'contaminated' by a contribution from an antiphase operator. Indeed, it is

the essence of selective spin-locking that the formation of antiphase magnetization is inhibited, in so far as various cross-correlation terms can be neglected (Burghardt et al., 1992). In fact when the locking field is orthogonal to the static field B_0, we have (Blicharski, 1972; Peng and Wagner, 1992):

$$\rho^t_{LOCK}(I_x^A) = \rho^t_{LOCK}(I_y^A) = \rho^t_{LOCK} \text{ (in-phase)}$$

$$= \gamma^4 \hbar^2 (8r_{AX}^6)^{-1} \{5J_{AX}(\omega_e) + (9/2)J_{AX}(\omega_0 - \omega_e) + (9/2)J_{AX}(\omega_0 + \omega_e) \tag{15}$$

$$+ 3J_{AX}(2\omega_0 - \omega_e) + 3J_{AX}(\omega_0 + \omega_e)\}$$

$$\rho^t_{LOCK}(2I_x^A I_z^X) = \rho^t_{LOCK}(2I_y^A I_z^X) = \rho^t_{LOCK} \text{ (antiphase)}$$

$$= \gamma^4 \hbar^2 (8r_{AX}^6)^{-1} \{J_{AX}(0) + 4J_{AX}(\omega_e) + (3/2)J_{AX}(\omega_0 - \omega_e) \tag{16}$$

$$+ (3/2)J_{AX}(\omega_0 + \omega_e) + 6J_{AX}(2\omega_0)\} + \rho_{MX} + \rho_{M'X} + \rho_{M''X} + ...$$

where ω_e is the amplitude of the radiofrequency field. Usually, we may assume because of our weak radiofrequency fields that the spectral densities are uniform over the range $\omega_0 \pm \omega_e$ and over the interval $2\omega_0 \pm \omega_e$. Since $J_{AX}(\omega_e) \approx J_{AX}(0)$, we obtain by comparison with Eqs. 1 and 2:

$$\rho^t_{LOCK}(\text{in-phase}) = \rho^t(\text{in-phase})$$

$$\rho^t_{LOCK}(\text{anti-phase}) = \rho^t(\text{antiphase}) \tag{17}$$

The expressions of Eqs. 13 and 15 are directly relevant to our measurements. Consider the rates ρ^t and ρ^t_{LOCK} of H^ε in Tyr[23], which feature a striking discrepancy (see Fig. 1). If we identify the proton H^ε with spin A in Eq. 2, and the coupling partner H^δ to spin X, it is obvious that X is subject to strong fluctuating dipolar fields originating from the H^β and $H^{\beta'}$ protons, which may therefore be identified with M and M' in Eq. 2. On the other hand, the rates ρ^t and ρ^t_{LOCK} of H^δ in Tyr[23] are rather similar. If in this case we identify the proton H^δ with spin A, its coupling partner X = H^ε is hardly subject to any fluctuating dipolar fields, since the H^β and $H^{\beta'}$ protons are too far away from H^ε to play the role of M and M'. Thus the fact that $\rho^t > \rho^t_{LOCK}$ for H^ε but that $\rho^t \approx \rho^t_{LOCK}$ for H^δ is consistent with the fact that the longitudinal relaxation rates fulfil the inequality $\rho(H^\delta) > \rho(H^\varepsilon)$.

In principle, a similar analysis can be made for an AMX three-spin system. It turns out that the eigenvectors of the Liouville matrix are rather complicated, so that we shall leave these details to be described in a later paper. This is why we shall not give a detailed discussion of the relaxation rates measured in Cys[30], which have been recapitulated in Fig. 2. We note in passing that there is a remarkable discrepancy between ρ^t and ρ^t_{LOCK} for H^α and for $H^{\beta'}$, but much less for H^β. Clearly, one has to be very careful in attempting to predict the ratio of the decay rates $1/T_2$ and $1/T_{1\rho}$ of transverse magnetization!

For both the Tyr[23] and Cys[30] systems, the double- and zero-quantum coherences have approximately the same decay rates. These rates, which were measured with selective methods (Nicula and Bodenhausen, 1993), are generally much faster than we anticipated. The relevant rates have been given elsewhere in terms of spectral densities of fluctuating dipolar and random fields (Macura et al., 1981; Ernst et al., 1987). In contrast to the preceding discussion, we assume here

that the spectral density function is of the form $J_{AX}(\omega_0) = 2\tau_c/(1 + \omega_0^2\tau_c^2)$. If we are in the slow motion limit, we expect the following ratios of the decay rates of the zero-, single- and double-quantum coherences of an isolated two-spin system:

$$\rho(ZQC) : \rho(SQC) : \rho(DQC) = 2 : 5 : 0. \tag{18}$$

Clearly, this is not compatible with the experimental results. We may assume once more that spin X is subject to dipolar interactions MX, M'X, M"X, ... This increases the relaxation rates $\rho(ZQC)$ and $\rho(DQC)$ by a contribution that is of the same order as $\rho(SQC)$. Thus we expect the following ratios in the slow motion limit

$$\rho(ZQC) : \rho(SQC) : \rho(DQC) = 7 : 5 : 5. \tag{19}$$

This is still not in good agreement with our hypothesis, so that further theoretical and experimental investigations are required.

CONCLUSIONS

The method described in this paper opens up an entirely new domain of investigation. We have illustrated how the selective methods that we recently introduced (Konrat et al., 1991; Boulat et al., 1992) can open the way to proton relaxation studies in macromolecules. This is the first time that one has access to such plentiful data about proton relaxation. In future work, it should be possible to pick up local variations of correlation times and spectral density functions in analogy to heteronuclear relaxation measurements (Palmer et al., 1991b; Peng and Wagner, 1992). We have offered a tentative explanation for the fact that, under certain conditions, transverse decay is found to be slower in the presence of spin-locking than under conditions of free precession, i.e. that $T_{1\rho}$ can be longer than T_2. This observation may help to explain the success of coherence transfer methods under spin-locked conditions, be it through our doubly selective method or through the more commonly used non-selective Hartmann–Hahn effect. In two- and higher-dimensional NMR of biomolecules, most experiments that involve heteronuclear magnetization transfer are based on combinations of pulses and free precession intervals, and therefore suffer from signal losses due to T_2 relaxation. Our observation that $T_{1\rho}$ is often longer than T_2 suggests that it might be of advantage to use cross-polarization techniques (Müller and Ernst, 1979) for the transfer of magnetization through heteronuclear scalar couplings.

ACKNOWLEDGEMENTS

REFERENCES

Bax, A., Ikura, M., Kay, L.E., Torchia, D.A. and Tschudin, R. (1990) *J. Magn. Reson.*, **86**, 304–318.

Blicharski, J.S. (1972) *Acta Physica Polonica A*, **41**, 223–236.

Boulat, B., Konrat, R., Burghardt, I. and Bodenhausen, G. (1992) *J. Am Chem. Soc.*, **114**, 5412–5414.

Brüschweiler, R. and Ernst, R.R. (1992) *J Chem. Phys.*, **96**, 1758–1766.

Burghardt, I., Konrat, R. and Bodenhausen, G. (1992) *Mol Phys.*, **75**, 467–486.

Clore, G.M., Szabo, A., Bax, A., Kay, L.E., Driscoll, P.C. and Gronenborn, A.M. (1990) *J. Am. Chem. Soc.*, **112**, 4989–4991.

Emsley, L. and Bodenhausen, G. (1989) *J. Magn. Reson.*, **82**, 211–221.

Emsley, L., Kowalewski, J. and Bodenhausen, G. (1990) *Appl. Magn. Reson* , **1**, 139–147.

Emsley, L. and Bodenhausen, G. (1992) *J. Magn. Reson.*, **97**, 135–148.

Ernst, R.R., Bodenhausen, G. and Wokaun, A. (1987) *Principles of Nuclear Magnetic Resonance in One and Two Dimensions*. Clarendon Press, Oxford.

Goldman, M. (1984) *J. Magn Reson.*, **60**, 437–452.

Kay, L.E., Torchia, D.A. and Bax, A. (1989) *Biochemistry*, **28**, 8972–8979.

Konrat, R., Burghardt, I. and Bodenhausen, G. (1991) *J. Am. Chem Soc.*, **113**, 9135–9140.

Kowalewski, J. (1990) *Ann. Rep NMR Spectrosc.*, **22**, 308–414.

Lipari, G. and Szabo, A. (1982) *J. Am. Chem. Soc.*, **104**, 4559–4570.

London, R.E. (1990) *J. Magn. Reson.*, **86**, 410–415.

Macura, S., Huang, Y., Suter, D. and Ernst, R R. (1981) *J Magn. Reson.*, **43**, 259–281.

Müller, L. and Ernst, R.R. (1979) *Mol Phys.*, **38**, 963–992.

Müller, N., Di Bari, L. and Bodenhausen, G. (1991) *J. Magn. Reson* , **94**, 73–81.

Nicula, S. and Bodenhausen, G. (1993) *J. Magn Reson. series A*, **101**, 209–214.

Palmer, III, A.G., Cavanagh, J., Wright, P.E. and Rance, M. (1991a), *J. Magn. Reson* , **93**, 151–170.

Palmer, III, A.G., Rance, M., Wright, P.E. (1991b) *J. Am Chem. Soc* , **113**, 4371–4380.

Peng, J.W., Thanabal, V. and Wagner, G. (1991a) *J. Magn. Reson.*, **94**, 82–100.

Peng, J.W., Thanabal, V. and Wagner, G. (1991b) *J. Magn. Reson.*, **95**, 421–427.

Peng, J.W. and Wagner, G. (1992) *J. Magn. Reson.*, **98**, 308–332.

Piantini, U., Sørensen, O.W. and Ernst, R.R. (1982) *J Am Chem Soc* , **104**, 6800–6801.

Rance, M., Sørensen, O.W., Bodenhausen, G., Wagner, G., Ernst, R.R. and Wüthrich, K. (1983) *Biochem. Biophys. Res. Commun.*, **117**, 479–481.

Vincent, S.J.F., Zwahlen, C. and Bodenhausen, G. (1992) *J. Am. Chem. Soc.*, **114**, 10989–10990.

Vold, R.L. and Vold, R.R. (1976) *J. Chem. Phys.*, **64**, 320–332.

Vold, R.L. and Vold, R.R. (1978) *Prog. Nucl Magn. Reson Spectrosc.*, **12**, 79–131.

Wagner, G. and Wüthrich, K. (1982) *J. Mol. Biol.*, **155**, 347–366.

Wagner, G., Bodenhausen, G., Müller, N., Rance, M., Sørensen, O.W., Ernst, R.R. and Wüthrich, K. (1985) *J. Am Chem. Soc.*, **107**, 6440–6446.

Wagner, G., Brühwiler, D. and Wüthrich, K. (1987) *J. Mol. Biol.*, **196**, 227–231.

Werbelow, L.G. and Grant, D.M. (1977) *Adv. Magn. Reson.*, **9**, 189–299.

Zwahlen, C., Vincent, S.J.F. and Bodenhausen, G. (1992) *Angew. Chem* , **104**, 1233–1236; *Angew. Chem. Int. Ed. Engl.*, **31**, 1248–1251.

Zwahlen, C., Vincent, S.J.F. and Bodenhausen, G. (1993) *Proceedings of the International Summer School of Physics 'Enrico Fermi'*, Varenna, in press.